Red and orange laser operation of Pr:KYF_4 pumped by a Nd:YAG/LBO laser at 469.1nm and a InGaN laser diode at 444nm

B. Xu,[1,2] F. Starecki,[1] D. Pabœuf,[3] P. Camy,[1,*] J. L. Doualan,[1] Z. P. Cai,[2] A. Braud,[1] R. Moncorgé,[1] Ph. Goldner,[4] and F. Bretenaker[3]

[1]*Centre de Recherche sur les Ions, les Matériaux et la Photonique (CIMAP), UMR 6252 CEA-CNRS-ENSICaen, Université de Caen Basse-Normandie, 14050 Caen, France*
[2]*Department of Electronic Engineering, Xiamen University, Xiamen 361005, China*
[3]*Laboratoire Aimé Cotton, CNRS-Université Paris Sud 11, 91405 Orsay, France*
[4]*Laboratoire de Chimie de la Matière Condensée de Paris, UMR CNRS-7574, Chimie-Paristech 75005 Paris, France*
**patrice.camy@ensicaen.fr*

Abstract: We report the basic luminescence properties and the continuous-wave (CW) laser operation of a Pr^{3+}-doped KYF_4 single crystal in the Red and Orange spectral regions by using a new pumping scheme. The pump source is an especially developed, compact, slightly tunable and intra-cavity frequency-doubled diode-pumped Nd:YAG laser delivering a CW output power up to about 1.4 W around 469.1 nm. At this pump wavelength, red and orange laser emissions are obtained at about 642.3 and 605.5 nm, with maximum output powers of 11.3 and 1 mW and associated slope efficiencies of 9.3% and 3.4%, with respect to absorbed pump powers, respectively. For comparison, the Pr:KYF_4 crystal is also pumped by a InGaN blue laser diode operating around 444 nm. In this case, the same red and orange lasers are obtained, but with maximum output powers of 7.8 and 2 mW and the associated slope efficiencies of 7 and 5.8%, respectively. Wavelength tuning for the two lasers is demonstrated by slightly tilting the crystal. Orange laser operation and laser wavelength tuning are reported for the first time.

OCIS codes: (140.5560) Pumping; (140.5680) Rare earth and transition metal solid-state lasers; (140.7300) Visible lasers.

References and links

1. T. Gün, P. Metz, and G. Huber, "Power scaling of laser diode pumped Pr^{3+}:$LiYF_4$ cw lasers: efficient laser operation at 522.6 nm, 545.9 nm, 607.2 nm, and 639.5 nm," Opt. Lett. **36**(6), 1002–1004 (2011).
2. B. Xu, P. Camy, J. L. Doualan, Z. Cai, and R. Moncorgé, "Visible laser operation of Pr^{3+}-doped fluoride crystals pumped by a 469 nm blue laser," Opt. Express **19**(2), 1191–1197 (2011).
3. P. Camy, J. L. Doualan, R. Moncorgé, J. Bengoechea, and U. Weichmann, "Diode pumped Pr^{3+}:KY_3F_{10} red laser", Opt. Lett. 32 (11), 1462–1464 (2007) and U. Weichmann, J. Bengoechea, P Camy, JL Doualan, R Moncorgé - US Patent 8000,363 B2, Aug. 2011.
4. S. Khiari, M. Velazquez, R. Moncorgé, J. L. Doualan, P. Camy, A. Ferrier, and M. Diaf, "Red luminescence analysis of Pr^{3+} doped fluoride crystals," J. Alloy. Comp. **451**(1-2), 128–131 (2008).
5. Ph. Goldner, O. Guillot-Noel, G. Dantelle, M. Mortier, T. H. My, and F. Bretenaker, "Orange avalanche upconversion for high-resolution laser spectroscopy," Eur. Phys. J. Appl. Phys. B **37**(2), 161–168 (2007).
6. F. Reichert, F. Moglia, D.-T. Marzahl, P. Metz, M. Fechner, N.-O. Hansen, and G. Huber, "Diode pumped laser operation and spectroscopy of Pr^{3+}:LaF_3," Opt. Express **20**(18), 20387–20395 (2012).
7. Z. Xia, A. Arcangeli, R. Faoro, and M. Tonelli, "Luminescence study of the f-f transition of Pr^{3+} $^1D_2$ and $^3P_0$ states in KYF_4 crystals and powders," Optoelectronics & Adv. Mater. **5**(4), 336–340 (2011).
8. D. Parisi, S. Veronesi, and M. Tonelli, "Effects of polarized excitation on the ^3P_J manifolds emission in KYF_4 Pr^{3+} single crystal," Opt. Mater. **34**(2), 410–413 (2011).
9. J. Klein, F. Beil, and T. Halfmann, "Robust population transfer by stimulated raman adiabatic passage in a Pr^{3+}:Y_2SiO_5 crystal," Phys. Rev. Lett. **99**(11), 113003 (2007).
10. M. P. Hedges, J. J. Longdell, Y. Li, and M. J. Sellars, "Efficient quantum memory for light," Nature **465**(7301), 1052–1056 (2010).

#181286 - $15.00 USD Received 5 Dec 2012; revised 18 Jan 2013; accepted 18 Jan 2013; published 27 Feb 2013

11. S. Renard, P. Camy, A. Braud, J. L. Doualan, and R. Moncorgé, "CaF_2 doped with Tm_{3+}: A cluster model," J. Alloy. Comp. **451**(1–2), 71–73 (2008).
12. D. Serrano, A. Braud, J.-L. Doualan, P. Camy, and R. Moncorgé, "Pr^{3+} cluster management in CaF_2 by codoping with Lu^{3+} or Yb^{3+} for visible lasers and quantum down-converters," J. Opt. Soc. Am. B **29**(8), 1854–1862 (2012).
13. B. Xu, P. Camy, J.-L. Doualan, A. Braud, Z. Cai, F. Balembois, and R. Moncorgé, "Frequency doubling and sum-frequency mixing operation at 469.2, 471, and 473 nm in Nd:YAG," J. Opt. Soc. Am. B **29**(3), 346–350 (2012).
14. E. Sani, A. Toncelli, M. Tonelli, and F. Traverso, "Growth and spectroscopic analysis of Tm, Ho: KYF_4," J. Phys. Condens. Matter **16**(3), 241–252 (2004).
15. T. H. Allik, L. D. Merkle, R. A. Utano, B. H. T. Chai, J. L. V. Lefaucheur, H. Voss, and G. J. Dixon, "Crystal growth, spectroscopy, and laser performance of Nd^{3+}:KYF_4," J. Opt. Soc. Am. B **10**(4), 633–637 (1993).
16. X. X. Zhang, P. Hong, M. Bass, and B. H. T. Chai, "Multisite nature and efficient lasing at 1041 and 1302 nm in Nd^{3+} doped potassium yttrium fluoride," Appl. Phys. Lett. **66**(8), 926–928 (1995).
17. J. Sytsma, S. J. Kroes, G. Blasse, and N. M. Khaidukov, "Spectroscopy of Gd^{3+} in KYF_4 - a system with several luminescent sites," J. Phys. Condens. Matter **3**(45), 8959–8966 (1991).
18. B. Y. Le Fur, N. M. Khaidukov, and S. Aleonard, "Structure of KYF_4," Acta Crystallogr. C **48**(6), 978–982 (1992).
19. M. J. Weber, *Handbook of Optical Materials* (CRC Press 2003)
20. T. Sandrock, T. Danger, E. Heumann, G. Huber, and B. Chai, "Efficient Continuous Wave-laser emission of Pr^{3+}-doped fluorides at room temperature," Appl. Phys. B **58**(2), 149–151 (1994).
21. M. Fibrich, H. Jelínková, J. Šulc, K. Nejezchleb, and V. Škoda, "Pr:$YAlO_3$ microchip laser," Opt. Lett. **35**(15), 2556–2557 (2010).

1. Introduction

Several Pr^{3+} doped fluoride crystals have been studied in the last years for their utilization as laser media. Particular interest lies in compact and directly diode pumped solid state laser systems operating in the visible range for various RGB laser applications such as large scale and miniature laser projectors.

Among all these materials, Pr^{3+} doped $LiYF_4$ is the one which led so far to the best laser performance [1,2] for a number of reasons which reside mainly in the specific spectroscopic characteristics of the Pr^{3+} active ion in this crystal together with its relatively low phonon energy. However, this crystal exhibits some drawbacks: i) the narrow line structure of its absorption forbids the use of standard laser diodes with non-specifically controlled emission wavelengths; ii) the narrow line structure and precise wavelengths of the emission transitions hardly allow for wavelength tuning. Consequently, there is still room for other Pr^{3+} doped materials with slightly less favorable absorption and emission cross sections but which present more favorable linewidths for diode pumping and laser tuning or offer new laser wavelengths for other particular applications. This is the case of Pr:KY_3F_{10}, which we described a few years ago [3]. This might be the case of Pr:CaF_2 [4] or Pr:PbF_2 [5] or Pr:LaF_3 [6], although these systems offer lower emission cross sections and led to less efficient laser action. This might be the case of Pr:KYF_4 whose spectroscopic properties were already partially presented in [4,7,8]. Indeed, as we shall see, despite less favorable transition cross sections and thermo-mechanical properties, this laser material presents broad absorption and emission features and is the only one, to our knowledge, which is able to lase at about 605.98 nm, which is a laser wavelength of interest for quantum information experiments [9,10]. There could be a possibility, as mentioned above, with Pr^{3+} doped fluorite crystals like Pr:CaF_2 or Pr:PbF_2 but by limiting the emission quenching resulting from the cross-relaxation energy transfers which occur in these materials, which can be achieved by breaking the ion clusters [11] responsible for these energy transfers by codoping the crystals with non-active ions like Y^{3+} [4] or Lu^{3+} [12].

In this paper, we first briefly describe the structural, thermo-mechanical and luminescence properties of Pr:KYF_4. In particular, new absorption and emission spectra have been registered in the blue/red spectral range both to clarify some past misunderstanding and to better account for the very particular structure of these spectra in the considered material. We focus then on the room-temperature continuous-wave laser operating conditions of Pr:KYF_4 in the red and orange spectral regions. For that purpose, an efficient alternative blue pump source, i.e., a CW Nd:YAG/LBO solid-state laser operating at about 469.1 nm, is employed in

#181286 - $15.00 USD Received 5 Dec 2012; revised 18 Jan 2013; accepted 18 Jan 2013; published 27 Feb 2013

this experiment [2,13]. For comparison, we also report the results obtained by using an InGaN blue diode laser with a maximum output power up to about 1 W at about 444 nm.

2. Structural and thermo-mechanical properties

Potassium yttrium tetrafluoride, KYF_4 has a trigonal non-centrosymmetric structure. The cell parameters are a = 14.06 Å and c = 10.103 Å. The cations are arramged an abc sequence is perpendicular to the c axis [14]. KYF_4 has been sometimes considered as a multisite host material [15,16] and sometimes as a disordered one [14,17,18]. According to the statement of disordered theory, the hexagonal unit cell of KYF_4 contains three cation layers, stacked according to the sequence abc. In each layer there are twelve cation positions. Four of these positions are occupied by Y^{3+} in each layer. The other eight positions are occupied by either Y^{3+} or K^+ according to a statistical distribution. So, when trivalent rare-earth dopants are introduced inside the matrix, they substitute for Y^{3+} ions with different environments. The consequence is that the local structure appears as slightly random and that, as will be shown in the following section, the optical absorption and emission spectra appear as broadband and multiline structures.

There are very few literature data on the growth characteristics and the thermo-mechanical properties of KYF_4. According to [16], the crystal melts around 800°C and grows incongruently, and according to [19], its refractive index should be around 1.42 (comparable to CaF_2) and its hardness is about 3 in Mohs scale. In fact, KYF_4 seems to have less favorable thermo-mechanical properties than the other fluorides. The argument is supported by Allik et al. [15] in their analysis on Nd:KYF_4. They found detrimental thermal effects at high powers, which implied weaker thermo-optical and thermo-mechanical properties of Nd:KYF_4 than Nd:YAG. A high laser threshold was also observed in Nd:KYF_4, which limits the use of KYF_4 as a rare earth doped host crystal. Sandrock et al. [20] further confirmed the weak and undesirable thermo-optical properties of Pr:KYF_4. By using an argon-ion laser as pump source, they obtained the first red laser emission at 642.5 nm. But they also found this material to be very sensitive to thermal stresses and cracks when it is pumped at higher powers.

3. Luminescence properties

As pointed out above, the spectroscopic properties of Pr:KYF_4 were already partly presented in [4,7,8]. Polarized absorption spectra were only reported between 420 and 500 nm, which is the region of interest for optical pumping around 445 nm (GaN laser diode), 469 nm (frequency-doubled Nd:YAG or Nd:GGG) or frequency-doubled OPSL (479 nm). A Judd-Ofelt (J.O.) analysis of the absorption spectra could be performed, however, based on complete although not reported absorption data, to derive branching ratios and radiative lifetimes and to calibrate some of the emission lines in cross-section unit [4]. The J.O. parameters derived from this J.O. analysis were found equal to $\Omega_2 = 3.92\text{x}10^{-20}$ cm^2, $\Omega_4 = 1.78\text{x}10^{-20}$ cm^2, $\Omega_6 = 7.94\text{x}10^{-20}$ cm^2. This was used [4] to derive a $^3P_0$ intrinsic radiative lifetime $\tau_r \approx 54$ µs and an effective one $\tau_{eff} \approx 72$ µs, for a measured fluorescence lifetime $\tau_f \approx 60$ µs, and a peak emission cross section at 605.4 nm of about 9 x 10^{-20} cm^2.

A very sharp, intense but unusual emission peak was also noticed, although not interpreted, at a wavelength of 594.4 nm [4,7,8]. It is unusual because it was never found in any other Pr-doped materials. This led to some confusion in the interpretation of the data [7,8]. It was thought, for instance, that the observed sharp emission line was an emission coming from the $^3P_0$ emitting level of Pr^{3+} in this material, whereas the rest of the emission spectrum observed between about 550 and 650 nm in the same excitation conditions (blue excitation between about 430 and 480 nm) arose from the $^1D_2$ level. Such assignment, however, would hardly make sense in a low-energy phonon material like KYF_4 where the non-radiative population of the $^1D_2$ level lying below the $^3P_0$ emitting one is probably very weak.

#181286 - $15.00 USD Received 5 Dec 2012; revised 18 Jan 2013; accepted 18 Jan 2013; published 27 Feb 2013

Thus, to definitely clarify that question, we have registered both time-resolved emission spectra and fluorescence decays following laser selective excitation at various excitation wavelengths. In particular, emission spectra and fluorescence lifetimes have been registered either by exciting our sample (the same sample 0.5%Pr:KYF_4 as the one used in Ref. [4]) at various excitation wavelengths across the absorption band extending in the blue from about 430 to 480 nm, and associated with the $^3H_4 \rightarrow {}^3P_{0,1,2}$, $^1I_6$ absorption transitions of Pr^{3+}, or across the absorption band (see in Fig. 1) extending in the red from about 550 to 620 nm and associated with a $^3H_4 \rightarrow {}^1D_2$ absorption transition. As shown in Fig. 2, the emission spectra obtained after excitation in the blue or in the red completely differ from each other and are associated with different single exponential fluorescence decays and emission lifetimes of about 56 µs and 460 µs, respectively, in perfect agreement with what is expected for $^3P_{0,1}$ and $^1D_2$ emission transitions, respectively.

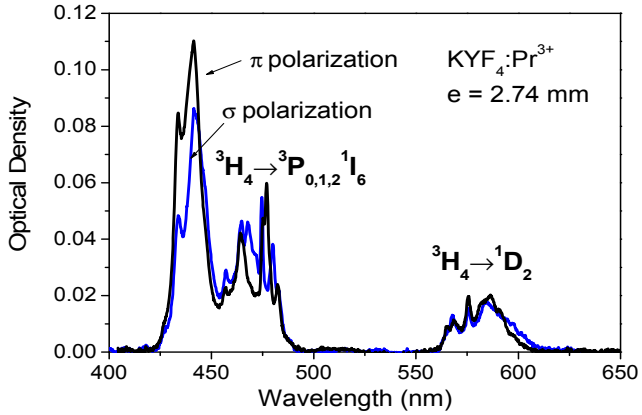

Fig. 1. Polarized absorption spectra in the blue/red spectral range.

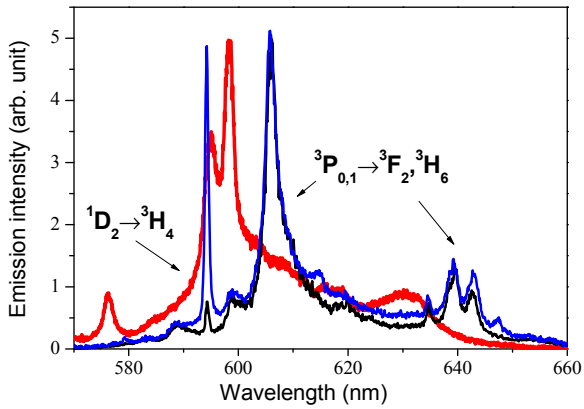

Fig. 2. Red emission spectra obtained after excitation in the blue at 442.5 nm (black), 457.9 nm (blue) and in the red at 569.5 nm (red).

In conclusion, the emission spectrum, which is obtained after excitation in the blue across the $^3H_4 \rightarrow {}^3P_{0,1,2}$, $^1I_6$ absorption bands occuring around 445, 469 and 480 nm, and which extends from 580 to 670 nm, is definitely assigned to $^3P_0 \rightarrow {}^3H_6$ and $^3P_0 \rightarrow {}^3F_2$ emission transitions. The contribution from the $^1D_2$ emitting level, which would be populated after a

#181286 - $15.00 USD Received 5 Dec 2012; revised 18 Jan 2013; accepted 18 Jan 2013; published 27 Feb 2013

$^3P_0 \rightarrow {}^1D_2$ transition because of multiphonon relaxations or cross-relaxation energy transfers, is perfectly negligible. The question remains, however, of the sharp emission peak observed around 594.5 nm. This line, indeed, is systematically observed, at low as well as at high Pr^{3+} concentration and does not depend on the history of the samples. According to our laser-selective excitation and time-resolved fluorescence measurements, this emission line, with a fluorescence lifetime identical to the rest of the emission spectrum, might be assigned to a minority but intrinsic Pr^{3+} site. X-rays diffraction data are being registered to try to elucidate that question.

4. Laser measurements

4.1 Laser experiments with a Nd:YAG/LBO 469.1 nm blue laser pump source

The laser crystal was pumped inside a two-mirror hemispherical resonator and the laser pump source was provided by an home-made diode-pumped and intracavity frequency-doubled CW Nd:YAG laser delivering up to 1.4 W at 469.1 nm [19]. The laser crystal was a 2.74 mm thick crystal having uncoated, flat, parallel and polished end-faces and it was mounted on a simple copper plate, without any additional cooling. The single pass absorption of the laser crystal is about 13% of the incident pump power at the 469.1 nm pump wavelength under the condition of no lasing.

A schematic of the experimental setup is shown in Fig. 3. The flat dichroic input mirror M1 had a high transmission (>97%) at the 469 nm (and also at the 444 nm) pump wavelength and it was highly reflective (>99.8%) at both red and orange emission wavelengths around 640 and 606 nm. The output mirrors M2 were plano-concave curved mirrors with a 50 mm radius of curvature and various transmissions at the different emission wavelengths. Because of its good beam quality ($M_x^2 = 1.3$, $M_y^2 = 2.0$), the pump laser was focused inside the laser crystal without any reshaping optics. The aspheric coupling lens, with a focal length of 50 mm, was chosen to optimize the overlap between the pump and cavity mode sizes inside the laser crystal. The calculated TEM_{00} mode waist radius inside the crystal was found equal to 34 m, whereas the pump spot radii in the x and y directions were found equal to about 40 and 35 μm.

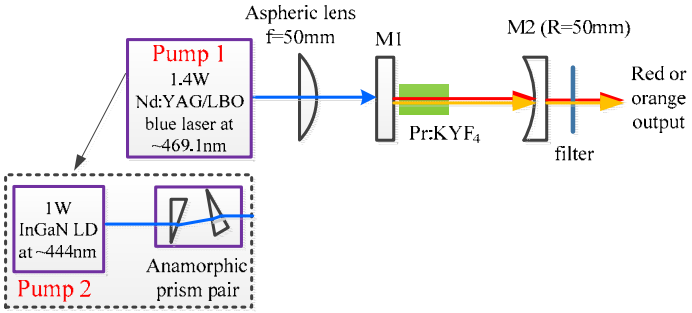

Fig. 3. Schematic laser experimental set-up based on a Nd:YAG/LBO (Pump 1) or a InGaN-LD (Pump 2) blue laser pump source.

With these conditions, red and orange laser action was achieved at 642.3 and 605.5 nm by using output mirrors with transmissions of 0.3% and 0.98%, respectively (see Fig. 4). Laser thresholds were reached for absorbed pump powers of about 40 and 130 mW, respectively. With maximum output powers of about 11.3 and 1 mW, this means slope efficiencies of about 9.3% and 3.4%. No laser effect was obtained with the other available output couplers (one with a transmission T = 1% around 640 nm and the other with T = 2% around 605 nm).

Laser wavelength tunability was achieved both in the red and the orange. It was obtained only by slightly tilting the laser crystal, which can be explained by a F-P etalon effect in the air gap between the laser crystal and the input mirror. The laser wavelength, measured with an ANDO 6315 Optical Spectrum Analyser with a spectral resolution of 0.05 nm, can be

#181286 - $15.00 USD Received 5 Dec 2012; revised 18 Jan 2013; accepted 18 Jan 2013; published 27 Feb 2013

shifted from 605.15 nm to 605.86 nm (see Fig. 5(a)-5(c)) for orange emission, and from 641.87 nm to 642.32 nm (see Fig. 5(d)-5(e)) for red emission.

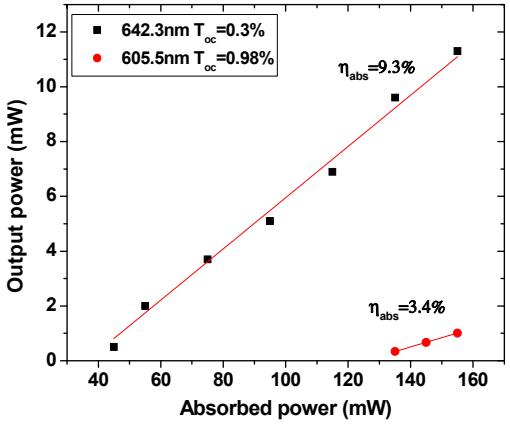

Fig. 4. CW laser output versus absorbed pump power curves obtained at 605.5 and 642.3 nm after pumping at 469 nm.

It is worthwhile to note that the tuning range allowed us to obtain orange laser emission around 605.8 nm which is the one required for quantum information experiments [9]. To the best of our knowledge, this is the first demonstration of continuous-wave laser operation in the orange and of laser wavelength tuning in this crystal. These preliminary laser results remain very modest. CW laser action, however, could be maintained for hours without significant power degradation. These modest laser results can be assigned both to the intrinsically less favorable thermo-mechanical properties of the host material but also to its not-yet optimized crystal growth. The laser sample indeed presented several cracks and bubbles. So, progress still can be made to improve the crystal quality and its laser performance. Furthermore, dual-wavelength laser emission at 605.55 and 642.2 nm has been also achieved by slightly tilting the laser crystal, which is recorded in Fig. 5(f).

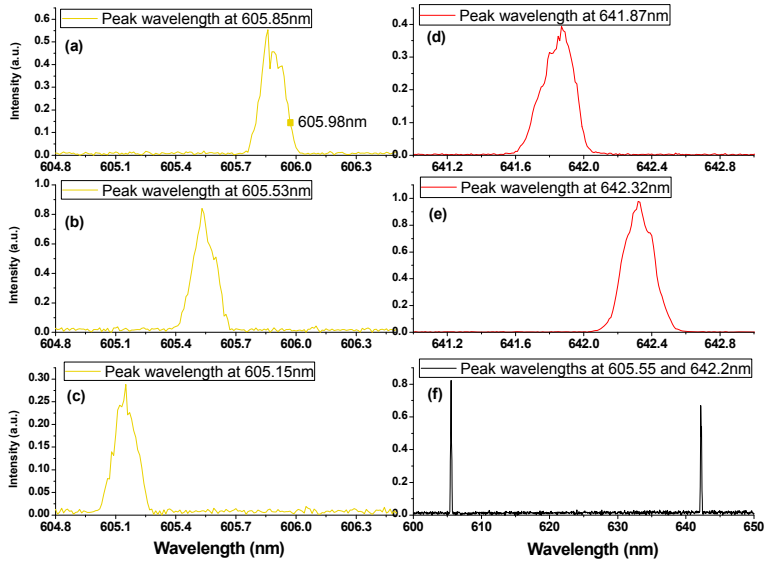

Fig. 5. Orange (a-c), red (d,e) laser wavelength tuning and dual-wavelength laser operation (f) obtained by tilting the laser crystal.

#181286 - $15.00 USD Received 5 Dec 2012; revised 18 Jan 2013; accepted 18 Jan 2013; published 27 Feb 2013

4.2 Laser experiments with a InGaN 444 nm blue diode laser pump source

Compared with the above home-made 469.1 nm Nd:YAG/LBO blue laser, the beam quality of the commercially available InGaN laser diodes is still very poor with reported beam propagation factors such as $M_x^2 = 1.4$, $M_y^2 = 5.8$ [1] or $M_x^2 = 2.9$, $M_y^2 = 4.1$ [21]. Therefore, it was necessary to reshape the diode laser beam before focusing it onto the laser crystal and, by using the same pump system as above, the pump spot radii in the x and y directions inside the crystal were found equal to about 46 and 30 μm, respectively.

The InGaN LD used in our experiments emits a linearly polarized light around 444 nm with a FWHM of about 0.4 nm and a full output power of nearly 1 W. The emission wavelength, however, varies from 442.8 nm to 444.7 nm when the output power is increased from 200 to 980 mW. According to the polarized absorption spectra of the material (see Fig. 1), the strongest absorption peak occurs at about 443 nm for both π (E//c) and σ (E//a) polarizations with a FWHM of around 2.5 nm, which almost perfectly coincides with the emission of the laser diode. As a matter of fact, compared with the pump at 469.1 nm, the absorbed pump single pass fraction is almost doubled with a value of about 24% without lasing. The Pr:KYF_4 laser cavity is the same plano-concave cavity as above.

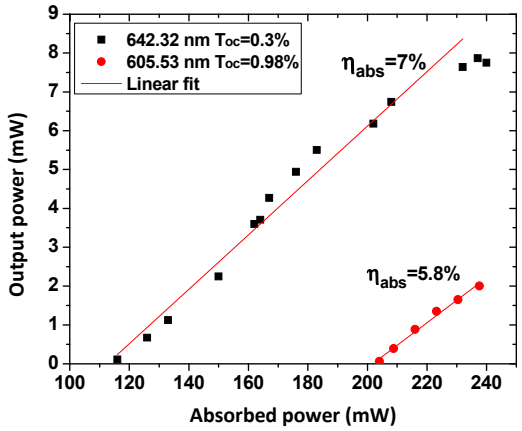

Fig. 6. CW laser output versus absorbed pump power curves obtained at red and orange laser wavelengths after pumping at about 444 nm.

The resulting laser output versus absorbed pump power curves are reported in Fig. 6. With the output coupler transmission of 0.3% for the red emission wavelength, true CW red laser emission is obtained with a threshold pump power of 116 mW, a maximum output power of 7.8 mW, and an associated laser efficiency of 7%. Changing the output coupler with transmission of 0.98% for the orange wavelength, we obtain the orange laser emission with a maximum output power of 2 mW, a threshold of 204 mW and a slope efficiency of 5.8%.

4. Conclusion

We have reported the CW laser operation at the red and orange laser wavelengths of about 642 and 605.5 nm of a Pr:KYF_4 crystal pumped by an especially developed continuous-wave Nd:YAG/LBO blue laser at around 469.1 nm with a maximum output power up to 1.4 W. Red and orange laser output powers of 11.3 mW and 1 mW have been obtained with corresponding optical-to-optical efficiencies of 2% and 0.3%. Wavelength tuning has been demonstrated by slightly tilting the crystal, from 605.15 to 605.85 nm, for the orange laser, and from 641.87 to 642.32 nm for the red laser. Dual-wavelength lasers at 605.55 and 642.2 nm has been also achieved by slightly moving the laser crystal. Finally, the same red and orange lasers are also reported for the first time by using a InGaN LD pump source emitting

#181286 - $15.00 USD Received 5 Dec 2012; revised 18 Jan 2013; accepted 18 Jan 2013; published 27 Feb 2013

at about 444 nm. In this case, maximum laser output powers of 7.8 mW and 2 mW at the red and orange laser wavelengths have been obtained with efficiencies of about 1.5%.

Acknowledgments

The authors wish to acknowledge the support from the French National Research Agency (ANR) within the framework of the FLUOLASE research program and the Chinese Scholarship Council (CSC) for the PhD scholarship of Mr. B. Xu. Thanks are also expressed to Prof. M. Tonelli for his loan of a crystal at the initial stage of this work.

#181286 - $15.00 USD Received 5 Dec 2012; revised 18 Jan 2013; accepted 18 Jan 2013; published 27 Feb 2013